

Endogenous Phosphotyrosine Signaling in Zebrafish Embryos*[§]

Simone Lemeer‡§, Rob Ruijtenbeek¶, Martijn W. H. Pinkse‡, Chris Jopling§, Albert J. R. Heck‡, Jeroen den Hertog§||, and Monique Slijper‡**

In the developing embryo, cell growth, differentiation, and migration are strictly regulated by complex signaling pathways. One of the most important cell signaling mechanisms is protein phosphorylation on tyrosine residues, which is tightly controlled by protein-tyrosine kinases and protein-tyrosine phosphatases. Here we investigated endogenous phosphotyrosine signaling in developing zebrafish embryos. Tyrosine phosphorylated proteins were immunoaffinity-purified from zebrafish embryos at 3 and 5 days postfertilization and identified by multidimensional LC-MS. Among the identified proteins were tyrosine kinases, including Src family kinases, Eph receptor kinases, and focal adhesion kinases, as well as the adaptor proteins paxillin, p130Cas, and Crk. We identified several known and some unknown *in vivo* tyrosine phosphorylation sites in these proteins. Whereas most immunoaffinity-purified proteins were detected at both developmental stages, significant differences in abundance and/or phosphorylation state were also observed. In addition, multiplex *in vitro* kinase assays were performed by incubating a microarray of peptide substrates with the lysates of the two developmental stages. Many of the *in vivo* observations were confirmed by this on-chip *in vitro* kinase assay. Our experiments are the first to show that global tyrosine phosphorylation-mediated signaling can be studied at endogenous levels in complex multicellular organisms. *Molecular & Cellular Proteomics* 6:2088–2099, 2007.

Embryonic development is tightly regulated, and numerous developmental processes like cell growth, differentiation, and migration are controlled by phosphotyrosine signaling, which is mediated by protein-tyrosine kinases and protein-tyrosine phosphatases. Improved knowledge about the identity of tyrosine phosphorylated proteins, their interacting proteins, and their involvement in signaling will improve our understanding of biological pathways and critical cellular processes. A first step toward elucidation of the critical signaling pathways is

the identification of tyrosine phosphorylated proteins in the developing embryo.

In recent years the availability of selective antibodies (1–4), targeted at tyrosine phosphorylated proteins, facilitated more global purification of these proteins and their binding partners, allowing identification by very sensitive LC-MS-based analysis of the proteins tryptic digests (1, 4, 5). Such approaches have been used for instance to study elegantly the temporal, global response to receptor stimulation. However, all of these data have been obtained from well defined cell systems under stimulated conditions. Although these data contribute well to our understanding of complex tyrosine phosphorylation-mediated signaling pathways, it is still unclear how they relate to *in vivo* processes. Therefore, *in vivo* studies are essential (6). Here we explored whether the above described technologies may be extended to perform a global analysis of *in vivo* signaling processes involved in zebrafish development. Zebrafish is now an established model organism for vertebrate development and human disease (7, 8). Zebrafish embryos are optically transparent, fertilization is external, and after 5 days of development most organs are formed, making it an ideal system to study development. Indeed by identifying mutations in key signaling molecules, direct insight into many signaling pathways involved in development was given (9, 10). However, a global insight in the post-translational modifications at the complex level of the whole organism has not been obtained.

Here we set out to evaluate whether the global analysis of endogenous tyrosine phosphorylation-mediated signaling processes involved in zebrafish development is feasible by analysis of their proteomes at two different developmental stages, 3 and 5 days postfertilization (dpf).¹ Embryogenesis of the zebrafish is a matter of days, and large numbers of zebrafish embryos can be obtained. A large amount of starting material is a prerequisite for proteomics studies and even more so for phosphoproteome analyses. Rigorous enrichment of tyrosine phosphorylated proteins is essential because ty-

From the ‡Department of Biomolecular Mass Spectrometry, Bijvoet Center for Biomolecular Research and Utrecht Institute for Pharmaceutical Sciences, Utrecht University, Sorbonnelaan 16, 3584 CA Utrecht, The Netherlands, §Hubrecht Institute, Uppsalalaan 8, 3584 CT Utrecht, The Netherlands, and ¶PamGene International B. V., Nieuwstraat 30, 5211 BJ 's Hertogenbosch, The Netherlands

Received, December 22, 2006, and in revised form, July 27, 2007
Published, MCP Papers in Press, August 14, 2007, DOI 10.1074/mcp.M600482-MCP200

¹The abbreviations used are: dpf, day(s) postfertilization; BLAST, basic logical alignment and research tool; IPI, International Protein Index; LTQ, linear ion trap; MS², tandem MS or MS/MS; MS³, neutral loss-dependent MS/MS/MS; NCBI-nr, National Center for Biotechnology Information non-redundant; RP, reversed phase; SCX, strong cation exchange; Fak, focal adhesion kinase; Eph, ephrin; E-value, Expectation value.

rosine phosphorylated proteins usually represent only 0.05% of the total amount of protein in a vertebrate cell (1, 2, 11). The analysis of a complex multicellular organism forms an extra challenge compared with *in vitro* cell lines comprising a single cell type. Therefore, we chose a number of enrichment steps consisting of immunoprecipitation of tyrosine phosphorylated proteins by a mixture of antibodies. Following proteolysis of the enriched proteins, the peptides were first separated by strong cation exchange chromatography after which the generated peptide fractions were further separated by reversed phase (RP) chromatography followed by mass spectrometric detection using an LTQ-FT-ICR mass spectrometer. This approach led to the identification of 800 immunoprecipitated proteins or their co-immunoprecipitating interacting partners, which are not necessarily tyrosine phosphorylated themselves (5). In addition, we identified 16 tyrosine phosphorylation sites and three serine phosphorylation sites on 14 proteins. The obtained *in vivo* results were further validated by immunoblotting and *in vitro* kinase assays using peptide microarray chips.

MATERIALS AND METHODS

Embryo Lysis and Immunoprecipitation—Embryos were grown until 3 or 5 dpf. At 3 dpf, embryos were de-yolked with de-yolk buffer (1/2 Ginzburg Fish Ringer) without calcium (12, 13). Subsequently embryos were lysed in buffer containing 50 mM Tris, pH 7.5, 150 mM NaCl, 1 mM EDTA, 1 mM sodium orthovanadate, 1% Nonidet P-40, 0.1% sodium deoxycholate, and protease inhibitor mixture (Complete Mini, Roche Diagnostics) and sonicated for 15 s. Lysates were centrifuged at $14,000 \times g$ to pellet cellular debris. Protein concentration was determined by a Quant kit (Amersham Biosciences/GE Healthcare) using the standard protocol. For each experiment, 10–25 mg of protein was used (corresponding to 1000–2000 embryo eq) as starting material from both samples. Lysates were pre-cleared on protein A-Sepharose beads (GE Healthcare) for 1 h at 4 °C to reduce non-specific binding of abundant proteins. Protein A beads were separated from the lysate by centrifugation. PY20 antibody (BD Transduction Laboratories) was incubated with each of the two lysates for 1 h followed by the addition of protein A/G Plus beads (Santa Cruz Biotechnology, Heidelberg, Germany) for 1 h. Finally agarose-conjugated pTyr-100 (Cell Signaling Technology, Danvers, MA) was added for overnight incubation. Precipitated proteins and complexes were washed extensively with HNTG buffer (50 mM Hepes, pH 7.4, 150 mM NaCl, 10% glycerol, and 0.1% Triton X-100). Bound proteins were eluted with 3 column volumes of 100 mM phenyl phosphate (Sigma) in PBS at room temperature. The buffer was exchanged to 25 mM ammonium bicarbonate, pH 8.5, and samples were concentrated using a Millipore spin column (5-kDa molecular mass cutoff) (Millipore, Amsterdam, The Netherlands). Eluates were diluted in 8 M urea, 25 mM ammonium bicarbonate, and Lys-C (Roche Diagnostics) was added. Digestion was performed for 4 h at room temperature. Samples were reduced with DTT at a final concentration of 2 mM at 56 °C; subsequently samples were alkylated with iodoacetamide at a final concentration of 8 mM at room temperature. The eluate was diluted to 2 M urea, 50 mM ammonium bicarbonate, and trypsin (Roche Diagnostics) was added. Digestion was performed overnight at 37 °C.

For paxillin and EphA4 reversed immunoprecipitation experiments, lysates were prepared and pre-cleared as described above. Paxillin (BD Transduction Laboratories) or EphA4 antibody (kindly provided by Dr. D. Wilkinson, Division of Developmental Neurobiology, National

Institute for Medical Research, The Ridgeway, Mill Hill, London, UK) was incubated with each of the two lysates for 1 h followed by the addition of protein A/G Plus beads for overnight incubation. Precipitated proteins were washed extensively with HNTG buffer. Bound proteins were eluted by boiling the beads in $2 \times$ sample buffer for 5 min at 95 °C.

Immunoblotting—For immunoblotting experiments, lysate and eluates from the immunoprecipitations were obtained as described above. Lysates (40 μ g, corresponding to 5 embryo eq) and immunoprecipitates (corresponding to 75 embryo eq) were subjected to SDS-PAGE and blotted. After transfer the membrane was stained with Coomassie Blue stain to verify equal loading of the lysates. Subsequently the PVDF membrane was blocked with 2% BSA and then incubated with the corresponding antibodies against phosphotyrosine (PY20), pSrc418 (both from BioSource Technologies), actin (Sigma), EphA4, and paxillin followed by the horseradish peroxidase-conjugated secondary antibody. The membranes were subjected to detection by enhanced chemiluminescence.

SCX Chromatography—Strong cation exchange was performed using a Zorbax BioSCX-Series II column (0.8-mm inner diameter \times 50-mm length; particle size, 3.5 μ m), a Famos autosampler (LC Packings, Amsterdam, The Netherlands), a Shimadzu LC-9A binary pump, and an SPD-6A UV detector (Shimadzu, Tokyo, Japan). Prior to SCX chromatography, protein digests were desalted using a small plug of C₁₈ material (3M Empore C₁₈ extraction disk) packed into a GELoader tip as described previously (14). The eluate was dried completely by vacuum centrifugation and subsequently reconstituted in 20% acetonitrile, 0.05% formic acid. After injection, the first 10 min were run isocratically at 100% solvent A (0.05% formic acid in 8:2 (v/v) water/acetonitrile, pH 3.0) followed by a linear gradient of 1.3% min⁻¹ solvent B (500 mM NaCl in 0.05% formic acid in 8:2 (v/v) water/acetonitrile, pH 3.0). A total number of 25 SCX fractions (1 min each, *i.e.* 50- μ l elution volume) were manually collected and dried in a vacuum centrifuge.

On-line Nanoflow Liquid Chromatography FT-ICR-MS—Nanoflow LC-MS/MS was performed by coupling an Agilent 1100 HPLC system (Agilent Technologies, Waldbronn, Germany) to a 7-tesla LTQ-FT-ICR mass spectrometer (Thermo Electron, Bremen, Germany) as described previously (15). Dried fractions were reconstituted in 10 μ l of 0.1 M acetic acid and delivered to a trap column (AquaTM C₁₈, 5 μ m, Phenomenex, Torrance, CA; 20 mm \times 100- μ m inner diameter, packed in-house) at 5 μ l/min in 100% solvent A (0.1 M acetic acid in water). Subsequently peptides were transferred to an analytical column (ReproSil-Pur C₁₈-AQ, 3 μ m, Dr. Maisch GmbH, Ammerbuch, Germany; 25 cm \times 50- μ m inner diameter, packed in-house) at \sim 150 nl/min in a 50-min gradient from 0 to 40% solvent B (0.1 M acetic acid in 8:2 (v/v) acetonitrile/water). The eluent was sprayed via emitter tips (made in-house) butt-connected to the analytical column. The mass spectrometer was operated in data-dependent mode, automatically switching between MS and MS² and neutral loss-driven MS³ acquisition. Full scan MS spectra (from *m/z* 300 to 1500) were acquired in the FT-ICR with a resolution of 100,000 at *m/z* 400 after accumulation to a target value of 500,000. The three most intense ions at a threshold above 5000 were selected for collision-induced fragmentation in the linear ion trap at a normalized collision energy of 35% after accumulation to a target value of 15,000. The data-dependent neutral loss settings were chosen to trigger an MS³ event after a neutral loss of either 24.5, 32.6, or 49 ± 0.5 *m/z* was detected among the five most intense fragment ions to determine serine and threonine phosphorylation.

Data Analysis—All MS² and MS³ spectra were converted to single DTA files using Bioworks 3.1. An in-house developed Perl script was used to assign for each MS³ spectrum the original and accurate parent mass from the full scan, enabling an accurate mass search for

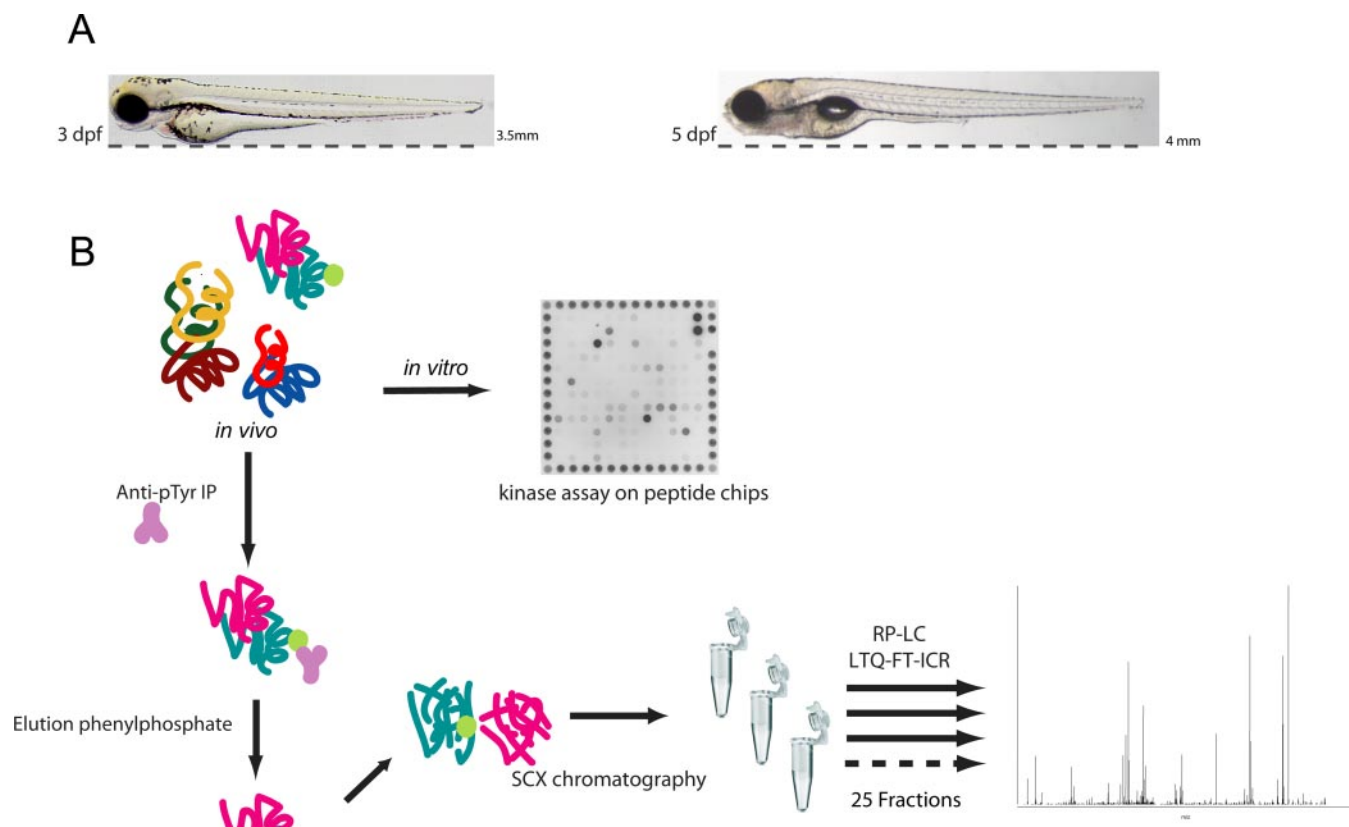


FIG. 1. Experimental scheme for the analysis of endogenous *in vivo* tyrosine phosphorylation during zebrafish development. *A*, lateral view of 3-dpf (*left*) and 5-dpf (*right*) zebrafish embryos. *B*, the lysates from 3- and 5-dpf embryos were used for direct *in vitro* kinase assays on a peptide microarray chip. Alternatively tyrosine phosphorylated proteins were immunoprecipitated by anti-Tyr(P) antibodies, and immunoprecipitated proteins were eluted from the antibodies using phenyl phosphate. A small portion ($1/25$) of the eluted proteins was subjected to SDS-PAGE and immunoblotted with five different antibodies. The majority of eluted proteins were digested, and the resulting peptides were separated first by SCX and subsequently (each of the obtained SCX fractions) further by nano-RP chromatography. Peptides were analyzed and identified by MS² and MS³ using a LTQ-FT-ICR mass spectrometer. *Anti-pTyr IP*, anti-phosphotyrosine immunoprecipitation.

these spectra as well. Eventually all MS² and MS³ spectra from each LC-MS run were merged to a single file, which was searched using the Mascot search engine (Matrix Science, London, UK, version 2.1.02) against the IPI zebrafish database (version 3.16; 46,700 entries) with carbamidomethylcysteine as fixed modification. Protein *N*-acetylation, methionine oxidation, and phosphorylation of serine, threonine, or tyrosine were specified as variable modifications. Trypsin was specified as the proteolytic enzyme, and up to two missed cleavages were allowed. The mass tolerance of the precursor ion was set to 15 ppm, and that of fragment ions was set to 0.9 Da. All phosphorylated peptides identified during Mascot searches were confirmed by manual interpretation of the spectra. Scaffold (version Scaffold-01_05_00, Proteome Software Inc., Portland, OR) was used to validate MS²-based peptide and protein identifications. Peptide identifications were accepted if they could be established at greater than 95.0% probability as specified by the Peptide Prophet algorithm (16). Protein identifications were accepted if they could be established at greater than 99.0% probability and contained at least two identified peptides. Protein probabilities were assigned by the Protein Prophet algorithm (16). A BLAST tool (www.ncbi.nlm.nih.gov/blast/) was used to identify protein names from their sequence. IPI zebrafish proteins annotated as “unknown” or “hypothetical” were searched for regions of local similarity between sequences in the NCBI-nr database, using a BLAST search engine, to extract supplementary information about this protein, such as putative function and protein

family. For this an in-house Perl script was developed that extracts the IPI zebrafish protein sequences from a FASTA database followed by an automated blast search against NCBI-nr. Chosen settings for BLAST (NCBI version 2.2.11) were an E-value cutoff off 1×10^{-4} and Blossum62; thus only proteins with a reasonable homology were retrieved and stored in a results file. Subsequently matches with an E-value between 1×10^{-100} and 1×10^{-200} (0.0) were regarded as close homologs (paralogs and orthologs cannot be ruled out with this method). Matches with higher E-values were used to deduce functional information or characteristics about the protein family.

In Vitro Kinase Assay—Microarray experiments were performed in triplicate using PamChip arrays (PamGene, 's Hertogenbosch, The Netherlands) run on a PamStation4 instrument (PamGene). This integrated microarray platform allows automated running of samples including incubation by pumping the sample up and down through the three-dimensional porous chip. The automated run includes data capturing by real time imaging (fluorescence signal development is read out by charge-coupled device imaging) and washing (17–20). A PamChip consists of four identical peptide microarrays, which run four samples in parallel during an experiment. The array used in this experiments comprised 144 different peptides (20). Each peptide represents a 15-amino acid sequence of which 13 residues are derived from a putative endogenous phosphorylation site. The peptide sequences used were derived from Swiss-Prot and/or Phosphobase databases and are provided in Supplemental Table 2. Two N-terminal

residues complete part of a spacer linking the phosphosite sequence to the solid support of the three-dimensional chip.

3- and 5-dpf embryos were lysed in buffer containing 50 mM Tris, pH 7.5, 150 mM NaCl, 1 mM sodium orthovanadate, 1% Nonidet P-40, 0.1% sodium deoxycholate, and EDTA-free protease inhibitor mixture (Sigma). Kinase activities in these lysates were analyzed in triplicate by applying 2.5–5 μ g of total protein in 25 μ l of kinase reaction buffer (Abl reaction buffer from New England Biolabs (Westburg, Leusden, The Netherlands) consisting of 100 mM MgCl₂, 10 mM EGTA, 20 mM DTT, and 0.1% Brij 35 in 500 mM Tris/HCl, pH 7.5). Additionally the kinase reaction buffer contained 12.5 μ g/ml fluorescein-labeled PY20 antibody against phosphotyrosine (Exalpha) and 400 μ M ATP (Sigma) for the PamChip peptide microarray. As control, kinase reaction buffer without ATP was used to detect background signal intensity. Prior to application of the sample, the chips were blocked using a solution of 2% BSA in water (Fraction V, Calbiochem) and washed two times with kinase reaction buffer. During a 60-min incubation at 30 °C, real time images were taken automatically every other 3 min. Images were analyzed by BioNavigator software (PamGene).

RESULTS

Identification of Endogenous Tyrosine Phosphorylated Proteins and Their Binding Proteins in Developing Zebrafish Embryos—We set out to identify tyrosine phosphorylated proteins in zebrafish embryos at 3 and 5 dpf. Illustrative pictures of zebrafish at 3 and 5 dpf are shown in Fig. 1A. A scheme of the experimental setup is provided in Fig. 1B: ~1500 embryos were lysed per experiment per time point. Phosphotyrosine-containing proteins were immunoprecipitated from these lysates using a mixture of anti-phosphotyrosine antibodies (PY20 and pTyr-100). Elution specificity of the bound proteins in this preparative setup was achieved by using phenyl phosphate. Immunoprecipitation efficiency was evaluated by immunoblotting using anti-phosphotyrosine antibody (PY20) as depicted in Fig. 2. The anti-Tyr(P) immunoblots shown in Fig. 2 reveal a clear enrichment of tyrosine phosphorylated proteins in the immunoprecipitated fractions for both 3- and 5-dpf zebrafish (Fig. 2, *Lysate versus IP*). Phenyl phosphate elution was efficient because no tyrosine phosphorylated proteins were detected on the beads after elution (Fig. 2, *Beads*). Reproducibly higher phosphotyrosine signals and different protein patterns were detected on the immunoblots of the 3- and 5-dpf embryos; lysates were loaded equally as verified by Coomassie staining of the immunoblot (data not shown).

Immunoprecipitated proteins from both stages were in-solution digested, and the resulting peptide mixture was analyzed by SCX-RP-LC-MS/MS. This multidimensional LC approach has the advantage that the separation of a complex peptide mixture is improved, allowing a more comprehensive analysis of all immunopurified proteins. In addition, SCX chromatography is known to enable targeted identification of phosphopeptides because most of these peptides elute simultaneously in the early fractions (21). In total we cumulatively identified over 800 proteins using the zebrafish IPI database as summarized in Supplemental Table 1 and

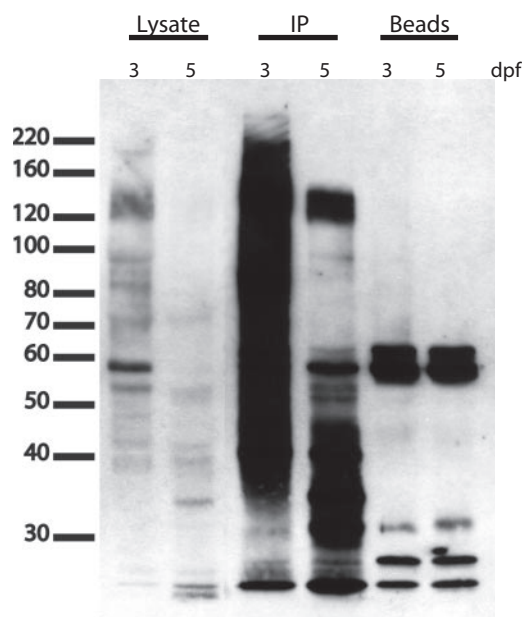


Fig. 2. Enrichment of tyrosine phosphorylated proteins from 3- and 5-dpf zebrafish embryos. An anti-Tyr(P) immunoblot showing enrichment of tyrosine phosphorylated proteins from 3- and 5-dpf embryo lysates using anti-Tyr(P) immunoprecipitation is shown. The 3-dpf embryos were deyolked prior to lysis. Lysates (corresponding to 5 embryo eq) and immunoprecipitates (corresponding to 75 embryo eq) were separated via SDS-PAGE, blotted, and probed with PY20. Detection was done using enhanced chemiluminescence and is depicted here. After specific elution, a clear enrichment of phosphorylated proteins is observed in the immunoprecipitates (*IP*). The boiled immunoaffinity beads do not give any significant signal (only light and heavy chains of the antibody), indicating that specific elution using phenyl phosphate was very efficient (*Beads*).

comprehensively described in the Scaffold file.² The zebrafish IPI database is not yet very well annotated as many proteins were annotated as unknown or hypothetical. To obtain an improved view of the potential function of these proteins, the functional annotations of many of the proteins were elucidated using BLAST searches and sequence alignments. We identified a large set of tyrosine kinases, which are expected to be phosphorylated on tyrosine (Table I). In addition, we identified adaptor proteins that may be phosphorylated on tyrosine themselves or that co-immunoprecipitate with tyrosine phosphorylated proteins (Table I). We used relatively mild lysis conditions that do not disrupt protein complexes and therefore allowed identification of co-immunoprecipitating proteins. Among the 800 identified proteins a large number of proteins were annotated as yolk, ribosomal, cytoskeleton, histone, and other highly abundant “housekeeping” proteins. It is well known that a targeted pulldown approach for tyrosine phosphorylated proteins can be hampered by the concomitant pulldown of highly abundant proteins.

We focused on the large set of tyrosine kinases and asso-

² M. Slijper, personal communication.

TABLE I
Identified phosphotyrosine signaling proteins in 3- and 5-dpf zebrafish embryos.

Proteins from 3- and 5-dpf zebrafish embryos that (co-)immunoprecipitated with anti-phosphotyrosine antibodies were identified with LC-FT-ICR-MS². These selected proteins are discussed in the text. A list of all identified proteins is given in Supplemental Table 1. The potential function of the protein was established by BLAST homology searches. The sequence coverage and cumulative number of detected unique peptides from three independent experiments are listed both for the 3- and 5-dpf samples. Identified proteins confirmed by immunoblotting are indicated in bold. More details can be found under "Materials and Methods" and in the supplemental Scaffold file.

Protein Name IPI database*	Blast†	IPI acc ID‡	Seq Cov %§		Cumm. Uni Pep		Phosphopeptide	
			3 dpf	5 dpf	3 dpf	5 dpf	3 dpf	5 dpf
Cytoplasmic tyrosine kinases								
Protein-tyrosine kinase	Yes	IPI00634359, IPI00487427	16	9	4	1		
Src protein	Src protein	IPI00489784	8	13	2	3		
Fyn Kinase	Fyn Kinase	IPI00481607, IPI00512478	6	9	1	1		
Src/Yes/Fyn					23 ^Δ	21 ^Δ	x	x
PREDICTED: similar to protein tyrosine kinase fer								
Focal adhesion kinase 1b	Focal adhesion kinase 1b	IPI00510461	12	8	26	13	x	x
Focal adhesion kinase 1a	Focal adhesion kinase 1a	IPI00488172	12	8	14	10	x	x
Dual specificity kinases								
Mitogen-activated protein kinase 14a/b	Mitogen-activated protein kinase 14a/b	IPI00481769	9	6	3	4	x	x
Mitogen-activated protein kinase 12	Mitogen-activated protein kinase 12	IPI00508892		15		6		x
Receptor tyrosine kinases								
Eph-like receptor tyrosine kinase rtk5	EphB4a	IPI00494777		5		2		
PREDICTED: similar to Ephrin type-B receptor 2 precursor								
	EphB2	IPI00505760, IPI00508574, IPI00512299, IPI00616026		6		4		
PREDICTED: similar to Ephrin type-B receptor 1 precursor								
101 kDa protein	EphA2	IPI00631901		6		3		x
Eph-like receptor tyrosine kinase 6	EphA2	IPI00493497		5		3		
106 kDa protein	EphB3	IPI00635201, IPI00496009, IPI00496327, IPI00633737	8	15	18	26		x
100kDa protein	EphA6	IPI00513436, IPI00632827, IPI00636497, IPI00742525		6		6		
novel protein similar to vertebrate EphA7	EphA7	IPI00499202		5		3		
EphA4 protein	EphA4a	IPI00506811, IPI00632580		5		4		x
Eph receptor EphA4b	EphA4b	IPI00505947		3		2		x
Eph receptor Eph3	EphB3	IPI00491575		3		2		
Adaptor proteins								
V-crk sarcoma virus CT10 oncogene homolog	Crk	IPI00487948, IPI00619445	8	17	4	11		x
Paxillin	Paxillin	IPI00499179		7		8		x
PREDICTED: similar to breast cancer anti-estrogen resistance 1								
98 kDa	p130Cas	IPI00482076	15	4	21	2	x	
	Cas-L	IPI00638454, IPI00636765, IPI00635056, IPI00627484	5		3		x	

* IPI protein name.

† Protein name obtained after NCBI BLAST.

‡ Accession number according to accession in IPI database.

§ Sequence coverage obtained from MS/MS peptide sequencing.

|| Cumulative number of unique peptides from three replicates obtained from MS/MS peptide sequencing.

Δ Cumulative number of unique peptides for Src, Fyn, and Yes together.

ciated signaling proteins. In Table I we list for these proteins the sequence coverage obtained by mass spectrometry and the number of cumulative unique peptides over three replicates. Although these numbers cannot be taken as an absolute measure of their abundance in the immunoprecipitate, significant differences were observed between the immunoprecipitates of 3 and 5 dpf. We note that many ephrin (Eph) receptor kinases were more easily detected at 5 dpf than at 3 dpf. The adaptor protein paxillin seems to be easier to detect in the immunoprecipitate of 3 dpf when compared with 5 dpf (see Table I). The sequence coverage we obtained for most tyrosine kinases and their adapter proteins remained mostly below 10%. Still we were able to detect 19 phosphorylation sites derived from 14 proteins in both stages whereby most of these were tyrosine phosphorylated sites. Four typical MS² spectra from the identified phosphopeptides are shown in Fig. 3; a summary of all phosphopeptide MS² and MS³ spectra is given in the supplemental data (Supplemental Spectra S1 and S2). Identified phosphorylation sites from both samples were manually confirmed and are shown in Table II along with their

Mascot score. The total number of tyrosine phosphorylation sites identified is not as high as in recently reported studies (1, 4, 5) due to the fact that all these earlier studies were on stimulated cells with relatively high phosphotyrosine levels compared with the endogenous levels in the whole organism as studied here.

We identified several components of focal adhesions at 3 and 5 dpf, including focal adhesion kinase (Fak) 1a and Fak1b. The Fak peptide YMEDSSYYK was shown to be phosphorylated on Tyr-7 or Tyr-8 (corresponding to Tyr-576 or Tyr-577 in human) in both the 3- and 5-dpf immunoprecipitates (Tables I and II). The doubly phosphorylated peptide was only detected in the 5-dpf sample. Two well known substrates of Fak, paxillin and p130Cas, were also detected, but only in the 3-dpf immunoprecipitate. In paxillin we identified QGVFLPEETPpY-SCPR (where pY is phosphotyrosine), corresponding to Tyr-31 in human (Fig. 3A and Table II) and thus a conserved tyrosine phosphorylation site from zebrafish to human. In p130Cas we identified four phosphopeptides, two tyrosine phosphorylated, one serine phosphorylated, and one doubly

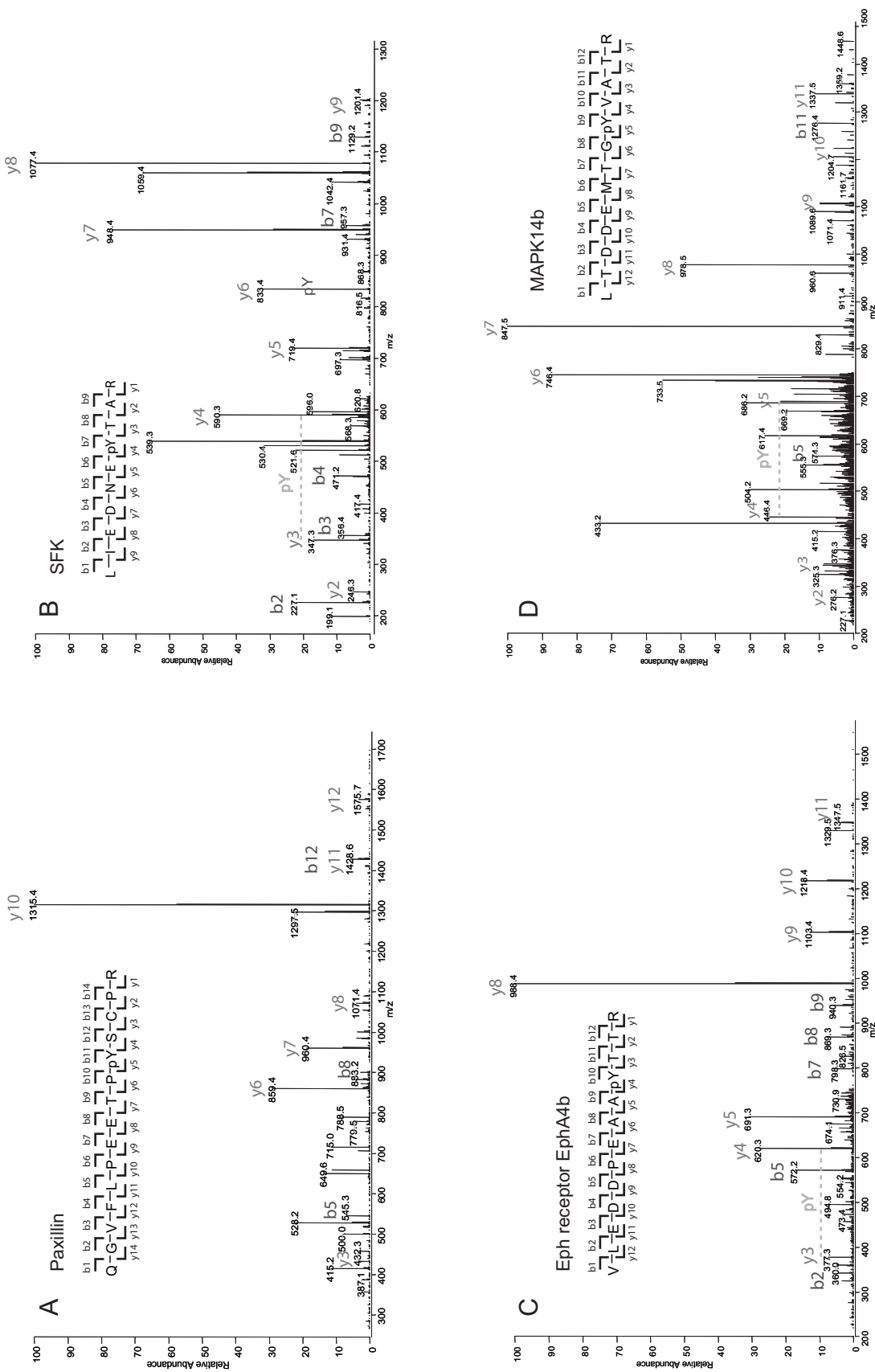


FIG. 3. MS² spectra from identified phosphopeptides. A, MS² spectrum of QGVFLPEETPpYSCPR from Paxillin. B, MS² spectrum of LIEDNEpYTAR from the Src family of kinases (SFK). C, MS² spectrum of VLEDDPEAApYTTR from Eph receptor EphA4b. D, MS² spectrum of LTDDEMTGpYVATR from mitogen-activated protein kinase 14b.

TABLE II
Identified *in vivo* phosphorylation sites

Phosphopeptides were identified using LC-LTQ-FT-ICR-MS² and LC-LTQ-FT-ICR-MS³ analysis. Some typical examples of these spectra are given in Fig. 3. Peptides indicated in bold are present as homolog on the peptide chip used for the *in vitro* kinase assay.

Phosphopeptides identified in 3 and 5 dpf immunoprecipitate					
Phosphopeptide*	Protein Name†	IPI acc nr‡	Mascot score (3 dpf/5 dpf)§	Human pSite	
AQGVpYDTPASR	Cas-L	IPI00638454, IPI00636765, IPI00635056, IPI00627484	43/36	NR	
LIEDNEpYTAR	Src Family Kinases	IPI00487427/ IPI00489784	63/55	Y418	
		P100634359/ IPI00481607/ IPI00507847			
LTDDEMTGpYVATR	Mitogen-activated protein kinase 14b	IPI00481769	60/72	Y181	
HTDDEMTGpYVATR	Mitogen-activated protein kinase 14a	IPI00494220	56/63	Y185	
VADEpYFIR	nicotinic acetylcholine receptor	IPI00497962	50/46	NR	
YMEDSSpYYK(ASK)	Focal adhesion kinase 1a/b	IPI00488172/ IPI00510461	23/49	Y576	
YMEDSSpYK	Focal adhesion kinase 1a/b	IPI00488172/ IPI00510461	22/52	Y577	
Phosphopeptides identified only in 3 dpf immunoprecipitate					
Phosphopeptide	Protein Name	IPI acc nr	Mascot score	Human pSite	
QGVFLPEETpYSCPR	Paxillin	IPI00499179	52	Y31	
RLpSASSTGSTR	p130Cas	IPI00482076	77	NR	
RQPEGQElpYDIPASLR	p130Cas	IPI00482076	68	NR	
GPPSGQElpYDTPPSVVDK	p130Cas	IPI00482076	55	NR	
RLpSAsSTGSTR	p130Cas	IPI00482076	33	NR	
QPEGQElpYDIPASLR	p130Cas	IPI00482076	33	NR	
Phosphopeptides identified only in 5 dpf immunoprecipitate					
Phosphopeptide	Protein Name	IPI acc nr	Mascot score	Human pSite	
QTDSEMTGpYVTR	Mitogen-activated protein kinase 12	IPI00508892	52	Y185	
VLEDDPEGTpYTTSGGK	EphA2	IPI00631901	39	Y772	
FLEDDPTDTPYTTSSLGGK	EphB3	IPI00635201	101	Y792	
VLEDDPEAApYTTR	EphA4b	IPI00505947	81	Y780	
VLEEDPDAApYTTR	EphA4a	IPI00506811, IPI00632580	50	Y778	
LLDQHNPEDELpS	Crk	IPI00487948, IPI00619445	42	NR	
YMEDSSpYpYKASK	Focal adhesion kinase 1a	IPI00488172	50	Y576/577	

* Phosphopeptide identified from MS/MS peptide sequencing.

† Protein name obtained after NCBI BLAST.

‡ Accession number according to accession in IPI database.

§ Sequence coverage obtained from MS/MS peptide sequencing.

|| Known human homologue of identified phosphorylation site. NR, no known human homologue reported.

phosphorylated (two Ser) (Tables I and II). None of the identified phosphopeptides from p130Cas have been previously reported, although for three of these sites (GPPSGQElpYDTPPSVVDK, RQPEGQElpYDIPASLR, and RLpSASSTGSTR where pS is phosphoserine) partial sequence homology exists in human p130Cas (22, 23).

Three members of the Src family of kinases, Fyn, Yes, and Src, were identified at both stages. Although these proteins have a high sequence homology we were able to identify at least one unique peptide for each protein at both stages, indicating that Fyn, Yes, and Src are all three immunoprecipitated (Table I). The total number of unique identified peptides in three replicates for the three Src family kinase members (Src, Fyn, and Yes) together is also given in Table I. The phosphopeptide LIEDNEpYTAR (autophosphorylation site Tyr-416 in human) was identified in 3- and 5-dpf embryos (Fig. 3B and Tables I and II).

Another quite abundant family of tyrosine kinases identified in our screen is the Eph family of receptor tyrosine kinases. We detected peptides of many of the known Eph receptors both in the 3- and 5-dpf immunoprecipitates (Table I). In the 5-dpf immunoprecipitate we also identified four phospho-

rylation sites on four different Eph receptors (Table II and Fig. 3C).

The adaptor molecule Crk was identified in both the 3- and 5-dpf immunoprecipitate samples (Table I). In the 5-dpf sample we were also able to identify a previously unreported serine phosphorylated peptide, LLDQHNPEDELpS (Table II). Mapk14a and Mapk14b were identified in the 3- and 5-dpf sample, including a phosphorylated site that has been previously reported for the human homolog (Tables I and II and Fig. 3D). Mapk12 was detected only in the 5-dpf sample, including a phosphorylated peptide (Tables I and II).

In Vitro Tyrosine Kinase Activities in Zebrafish Embryos—Concomitant with our *in vivo* screen for endogenous tyrosine phosphorylated proteins in zebrafish development, we performed an *in vitro* kinase assay using a peptide array (Fig. 4). Each microarray contained 144 peptides originating from putative tyrosine phosphorylation sites in known proteins. Peptides on the chip are primarily derived from human protein sequences, but nine phosphopeptides identified in our *in vivo* screen were present on the chip with likely sufficient sequence homology (Table II, indicated in bold, and Fig. 4D). A list of all peptides present on the chip can be found in Sup-

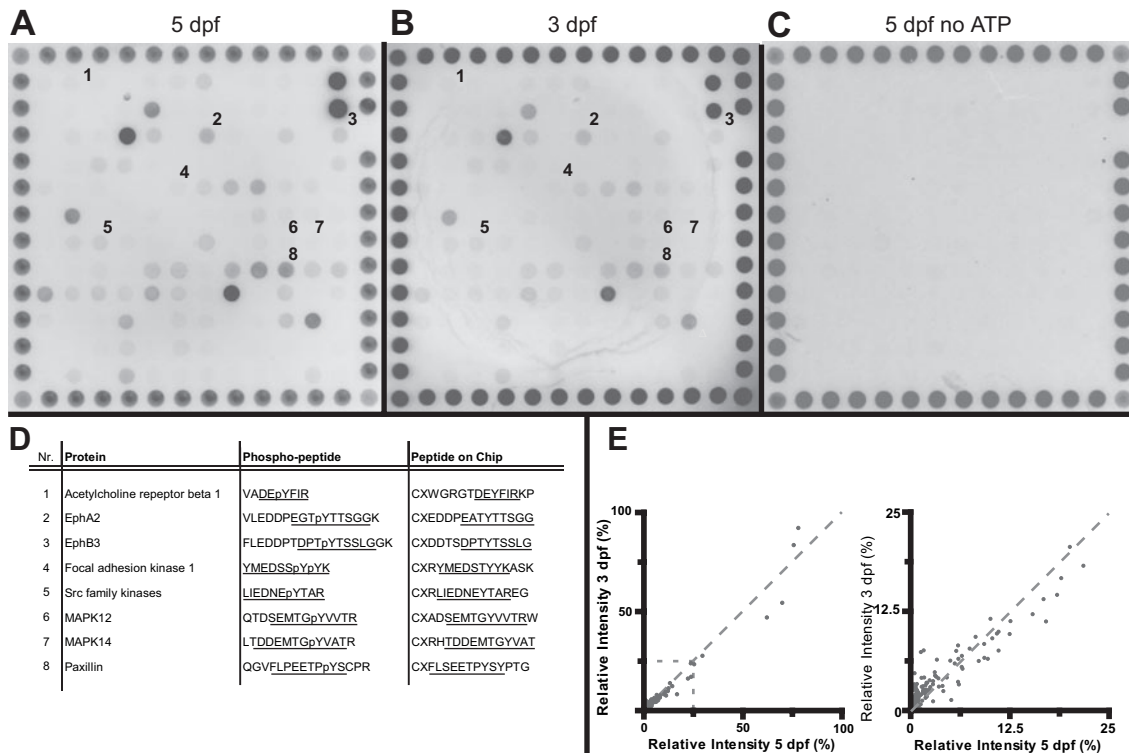


FIG. 4. *In vitro* kinase assays are consistent with *in vivo* phosphorylation. Kinase assays were performed using lysates of 3- and 5-dpf zebrafish embryos with arrays of 144 peptides encoding known tyrosine phosphorylation sites. Kinase reaction and detection are described under “Materials and Methods.” Pictures of the end points of the kinase reactions from 5 dpf (A), 3 dpf (B), and 5 dpf in the absence of ATP (C) are shown here. D, selection of peptides that were present on the chip. Numbers refer to position of the peptides on the chip in A and B. The identity of the proteins, the phosphopeptides detected by MS, and the sequence of the peptides on the chip are indicated. E, correlation graph between spot intensities after incubation with 5-dpf (x axis) and 3-dpf (y axis) embryo lysates. The panel on the right is an enlargement of the low intensity region on the left.

plemental Table 2. For our *in vitro* kinase assay we used lysates from 3- and 5-dpf zebrafish and performed the experiments in triplicate. These lysates were individually incubated on the peptide substrate chip in the presence of ATP. A fluorescently labeled anti-Tyr(P) antibody (PY20) was used to monitor tyrosine phosphorylation of the peptide substrates. Typical end point images are shown in Fig. 4 (A–C). All the peptide substrates identified by mass spectrometry that were found to be phosphorylated *in vivo* were phosphorylated *in vitro* both after incubation with 3- and 5-dpf lysates (Fig. 4, A and B). Especially peptides derived from paxillin, EphA2, EphB3, and the Src family kinases demonstrated a high *in vitro* phosphorylation signal. In the negative control (Fig. 4C) without ATP, no phosphorylation was detected, revealing that the signals in Fig. 4, A and B, were generated by kinase activity present in the lysates. The relative signal of *in vitro* peptide phosphorylation was corrected for background, and the 5-dpf spot intensities were plotted against the 3-dpf spot intensities (Fig. 4E). Spot intensities from both stages did not show significant differences, indicating similar kinase activities in both 3- and 5-dpf lysates. In summary, the detection of protein tyrosine phosphorylation at 3 and 5 dpf by mass spectrometry was confirmed by the results of this *in vitro*

phosphorylation assay, showing that indeed concomitant kinase activities are present, thus revealing the complementarities of these two methods.

Validation of Protein Tyrosine Phosphorylation by Immunoblotting—To further validate the *in vivo* mass spectrometry results, we used immunoblotting. Anti-Tyr(P) immunoprecipitates were blotted and probed with antibodies specific for proteins identified by mass spectrometry, notably paxillin, Src, and Eph receptor, with actin as control (Fig. 5). The blot probed with the paxillin antibody showed a decreased signal in the 5-dpf lysate compared with the 3-dpf lysate. A clear paxillin signal was observed in the 3-dpf eluate from the immunoprecipitation but not in the 5-dpf immunoprecipitate (Fig. 5A), which is in line with the fact that we detected paxillin with more unique peptides and higher sequence coverage at 3 dpf than at 5 dpf (Table I). The pSrc418 antibody gave a clear signal in the 3- and 5-dpf lysates and in the immunoprecipitates, showing tyrosine phosphorylation. However, there was a significant shift in the one-dimensional gel both in the lysates and the immunoprecipitate (see Fig. 5B). This shift may result from cross-reactivity with other Src family kinase members (Fig. 5B). The EphA4 antibody gave a signal in both the 3- and 5-dpf lysates, showing higher intensity for the 3-dpf

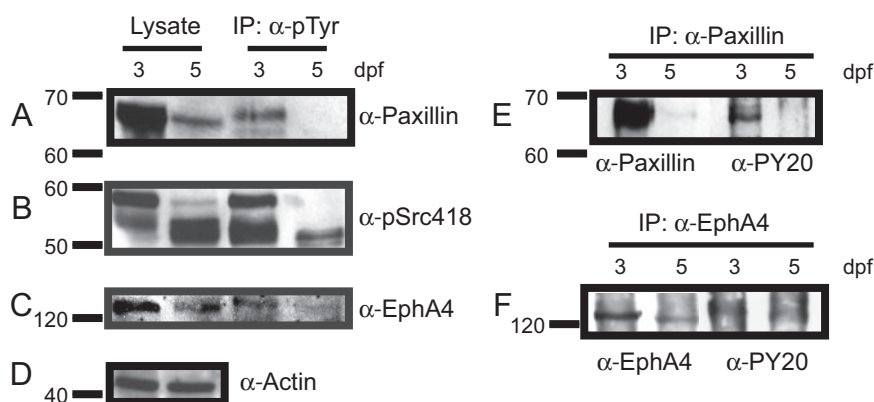


FIG. 5. **Validation of tyrosine phosphorylation of selected proteins by immunoblotting.** Zebrafish embryos were lysed at 3 or 5 dpf and immunoprecipitated with anti-Tyr(P) antibodies (α -pTyr; A–D). Immunoprecipitated proteins were specifically eluted with phenyl phosphate. Lysates (corresponding to 5 embryo eq) and immunoprecipitates (IP) (corresponding to 75 embryo eq) were subjected to SDS-PAGE and blotted. Blots were probed with the indicated antibodies: A, paxillin; B, pSrc418; C, EphA4; D, actin. For reverse immunoprecipitations (E and F), 3- and 5-dpf zebrafish embryos were lysed, and immunoprecipitation was performed with anti-paxillin (E) or anti-EphA4 (F) antibody. Immunoprecipitates (corresponding to 75 embryo eq) were subjected to SDS-PAGE and blotted. Blots were probed with the corresponding antibody, anti-paxillin (E) or EphA4 (F), to detect immunoprecipitation of the protein of interest. Subsequently blots were stripped and probed with anti-phosphotyrosine antibody. Detection was performed by enhanced chemiluminescence.

sample (Fig. 5C). This was also reflected in the immunoprecipitates of the 3- and 5-dpf samples. A slight shift in mass was observed in the immunoprecipitates, indicative for phosphorylation, although the signals were low. The actin antibody, which was used as control, gave equal signals in the lysates from both 3- and 5-dpf embryos, indicating equal loading.

We performed reverse immunoprecipitation experiments to corroborate tyrosine phosphorylation on paxillin and EphA4 (Fig. 5, E and F, respectively). Anti-paxillin immunoprecipitates were blotted and probed with paxillin and subsequently with phosphotyrosine (PY20) antibody. Fig. 5E shows that paxillin was indeed immunoprecipitated from the 3-dpf lysate. The amount of paxillin in the 5-dpf immunoprecipitate was much lower, which is in line with the paxillin expression profile in the lysates (Fig. 5A). After reprobing the blot with phosphotyrosine antibody we could only detect a tyrosine phosphorylation of paxillin in the 3-dpf sample but not in the 5-dpf sample, showing that paxillin is indeed phosphorylated in 3-dpf embryos.

The EphA4 immunoprecipitates were first probed with EphA4 antibody. EphA4 was readily immunoprecipitated from both 3- and 5-dpf lysates (Fig. 5F). However, the EphA4 signal was higher in the 3-dpf immunoprecipitate (Fig. 5F). After reprobing the blot with phosphotyrosine antibody we could detect a faint band in the 3-dpf immunoprecipitate that shows a mass shift compared with the EphA4 immunoblot that was indicative for its phosphorylation.

DISCUSSION

Here we examined tyrosine phosphorylation-mediated signaling during zebrafish development *in vivo* by mass spectrometry-based proteomics and complementary *in vitro* kinase assays with peptide substrate micro-arrays. We

performed our analyses on zebrafish embryos at 3 and 5 days postfertilization. The protein tyrosine phosphorylated subproteome was targeted in our analyses using anti-phosphotyrosine affinity purification (1, 4, 5). It is known that enrichment is essential, otherwise tyrosine phosphorylated proteins are present at undetectable levels (24). We explored successfully whether these well described methods can also be adopted to investigate tyrosine phosphorylation-mediated signaling in whole vertebrate organisms under natural, *i.e.* non-stimulated, conditions. Notably when there is no artificial stimulation as in the *in vivo* experiment described here, tyrosine phosphorylation is under strict regulation of protein-tyrosine kinases and protein-tyrosine phosphatases, resulting in extremely low endogenous levels of tyrosine phosphorylated proteins. Additionally by the nature of our experiments, localized tyrosine phosphorylation events in the whole organism become “diluted” compared with *in vitro* experiments using single cell types. For the large scale analyses of tyrosine phosphorylation, mostly cultures of single cell types are taken, comprising typically 10^8 – 10^9 cells per experiment (5, 24, 25). In our experiment we took 1000–2000 embryo eq, which contain a heterogenous cell population. Still with our approach, we detected 16 interesting tyrosine phosphorylation sites. This compares very well with, for example, recent results with analyses on cultured cells that overexpress ErbB2 where eight tyrosine phosphorylation sites were detected after treatment with Herceptin (24).

Immunoblot analysis showed that our immunoprecipitation approach was successful; a clear enrichment of tyrosine phosphorylated proteins was observed for both stages (Fig. 2). Although protein tyrosine phosphorylation seems to be reproducibly higher in the 3-dpf embryos, this observation was not supported by a higher amount of tyrosine phospho-

rylated proteins or phosphopeptides detected in our MS analysis. It should be noted that 3-dpf embryos still contain a higher proportion of yolk proteins. Despite removal of the yolk, many yolk proteins, predominantly vitellogenins, are still present in proteomic profiles of early zebrafish embryos (26). These vitellogenins are notoriously sticky proteins that may bind to the antibody and interfere with anti-Tyr(P) immunoprecipitation and immunoblotting.

Using extensive peptide separation methodologies with SCX and nano-RP chromatography coupled to LTQ-FT-ICR-MS/MS we identified over 800 proteins in the immunoprecipitate, containing a smaller interesting subset of tyrosine kinases and adaptors/substrates that are likely to play a major role in developmental processes. Moreover on these interesting proteins we were able to identify 19 phosphorylation sites of which several were not reported previously. We focus our discussion on several of these more interesting tyrosine kinases and their substrate/adaptor proteins.

Focal Adhesion Signaling—Focal adhesion proteins form a link between the extracellular matrix and the actin cytoskeleton. They play an important role in the transduction of adhesion and growth factor signals. Mouse embryos deficient in Fak or paxillin die early, illustrating the importance of focal adhesions in development (10, 27). Fak is a non-receptor tyrosine kinase that, in association with Src, phosphorylates paxillin at Tyr-31 (28). Zebrafish have two Fak genes, *fak1a* and *fak1b*, that are both expressed during early development. Tyrosine phosphorylation of Tyr-576/Tyr-577, which is important for catalytic activation, has also been observed in early developmental stages in zebrafish (29). We identified Fak1a and Fak1b in both 3- and 5-dpf samples. Tyrosine phosphorylation at Tyr-567 and Tyr-577 was detected in our proteomics screen and could be confirmed by the *in vitro* kinase assay (Fig. 4, A and B).

Paxillin, another major constituent of focal adhesions, binds many proteins that are involved in changing the actin cytoskeleton, which is necessary for cell motility events associated with development. Paxillin has been described as one of the major tyrosine phosphorylated proteins in embryonic development (30). In our proteomics screen paxillin was identified in the 3-dpf embryo with eight cumulative unique peptides, whereas it was not detected in the immunoprecipitate of the 5-dpf sample. Furthermore we identified the *in vivo* tyrosine phosphorylation of Tyr-31 (Tables I and II and Fig. 3A) in the 3-dpf embryo; this site is known to become phosphorylated in response to cell adhesion (28).

Immunoblot analysis with a paxillin antibody validated that phosphorylated paxillin is immunoprecipitated from the 3-dpf lysates and showed that expression is reduced in 5-dpf embryos compared with 3-dpf embryos (Fig. 5A). In the reverse immunoprecipitation experiment, it was shown that paxillin could be immunoprecipitated from the 3-dpf lysates but not from the 5-dpf lysates. Reprobing the blot with phosphotyrosine antibody clearly showed phosphorylation of paxillin in

the 3-dpf immunoprecipitate, whereas no phosphorylated paxillin could be detected in the 5-dpf immunoprecipitate (Fig. 5E). *In vitro* kinase assay experiments also confirmed tyrosine phosphorylation of paxillin at Tyr-31 (Fig. 4, A and B). However, the paxillin Tyr-31-containing peptide was phosphorylated by both the 3- and 5-dpf lysates. Focal adhesion kinase is still active in 5-dpf embryos, and therefore the paxillin Tyr-31 peptide (which is present in equal amounts on all chips) is also phosphorylated *in vitro*. *In vivo*, however, paxillin expression is reduced in 5-dpf embryos, suggesting that signaling of paxillin is regulated by expression levels rather than by phosphorylation. Together three independent methods confirm tyrosine phosphorylation of paxillin in 3-dpf embryos. Interestingly phosphorylation of Tyr-31 of paxillin creates an SH2 binding site for Crk (28, 31), a protein that was identified in our screen both in the 3- and 5-dpf samples.

In addition to Fak transphosphorylation and paxillin phosphorylation, recruitment of Src into the signaling complex also facilitates phosphorylation of p130Cas, which is a docking protein with well characterized roles in cell migration and invasion. Tyrosine phosphorylation of p130Cas is required for its binding to Crk, which induces signaling cascades leading to cell migration and extension (32). p130Cas was identified in the 3-dpf immunoprecipitate with 21 cumulative unique peptides, including some with detected phosphorylation sites. However, it was only detected with two cumulative unique peptides in the 5-dpf sample (Tables I and II), suggesting down-regulation. Expression differences of p130Cas could not be validated by immunoblot analysis because there is no zebrafish-specific antibody available. Together our results implicate that focal adhesion signaling is clearly dynamic from day 3 to 5 in zebrafish embryogenesis.

Src Family Kinases—The Src family kinases, Src, Fyn, and Yes, were detected in both immunoprecipitates, indicating that they likely are ubiquitously phosphorylated (Table I). Indeed we identified the autophosphorylation site (Tyr-418 in human) in the 3- and 5-dpf samples (Table II and Fig. 3B). This autophosphorylation site is responsible for the regulation of cell adhesion and activity of the kinase. Immunoblot analysis with a phosphospecific antibody recognizing the autophosphorylation site confirmed the presence of the phosphorylated Src in the lysates and the immunoprecipitates of both samples. Interestingly the immunoblot showed a significant shift in signal between the 3- and 5-dpf embryo lysates (Fig. 5B). The pSrc418 antibody cross-reacts with other Src family kinase members (Fyn or Yes) because this phosphorylation site is conserved throughout the family. The observed shift might indicate a switch in activity from one member of the family to the other between 3- and 5-dpf embryos. Based on the observed shifts in the immunoblot, Fyn may be present in the lower band, and Src or Yes may be present in the higher band. We were able to identify at least one unique peptide for each protein, showing that Src, Fyn, and Yes were immunoprecipitated at both stages. Due to the high homology be-

tween the three different family members, it was not possible to detect differential expression of the proteins in one of the stages. The role of the Src family kinases in cell signaling is well studied, but less is known about their role in embryonic development. Recent studies underline the importance of tyrosine kinases Fyn and Yes in the early embryonic development of zebrafish (33, 34). Our study shows that activity and phosphorylation of the Src family of kinases is still also high at later stages of development and reveals interesting dynamics in expression or post-translational regulation between the 3- and 5-dpf stages.

Eph Receptor Signaling—A large family of protein kinases identified in our proteomics assay is the Eph receptor family of protein-tyrosine kinases. Because Eph receptors and their ephrin ligands are membrane-bound, binding and activation requires cell-cell interaction (35). Bidirectional Eph receptor signaling is mainly responsible for the repulsion of neighboring cells or cellular processes, resulting in regulated cell migration, axon guidance, and tissue border formation (36, 37). Eph receptors are expressed in many tissues during development, and receptor activity has been shown to play important roles during development (37–39). The Eph receptor family contains more than 10 members of which we identified about eight (Table I) (Due to genome duplication, the zebrafish contains for some Eph receptors an a form and a b form that are not well annotated yet.). For several of these Eph receptors we identified known *in vivo* autophosphorylation sites (Table II), some of which were also detected in our *in vitro* kinase assay using the peptide array. We also detected phosphorylation of EphA4 both by MS and reverse immunoprecipitation experiments (Figs. 3C and 5E and Table II). Tyrosine phosphorylation of EphA4 has been shown by immunoblotting by Xu *et al.* (40) in earlier stage zebrafish embryo cells. Furthermore this site has been previously reported by Rush *et al.* (23) (PhosphoSite, Cell Signaling Technology). Our data suggest an important role for the various Eph receptors and their tyrosine phosphorylation and activation in the embryonic signaling pathways.

Conclusions—In summary, in this study tyrosine phosphorylation was analyzed using proteomics technologies in whole zebrafish *in vivo* to investigate signaling in zebrafish development at days 3 and 5 postfertilization. Differences in protein expression and in protein phosphorylation were observed, suggesting that notable signaling occurs intended for focal adhesion, cell adhesion, and cell sorting in axon guidance and in tissue border formation as well as for a number of other processes that are important in late embryogenesis. *In vivo* observed tyrosine phosphorylation could be complemented by detection of *in vitro* kinase activities and confirmed by Western blotting experiments. This shows the value of the complementary use of three technologies in the field of functional proteomics.

Acknowledgments—We thank Dr. David Wilkinson for the anti-EphA4 antibody. We are grateful to Dr. Bas van Breukelen for kind support with the BLAST searches.

* This work was supported by European Union Research Training Network HPRN-CT-2000-00085, Netherlands Organisation for Scientific Research Grant 015.001.131, and The Netherlands Proteomics Centre. The costs of publication of this article were defrayed in part by the payment of page charges. This article must therefore be hereby marked “advertisement” in accordance with 18 U.S.C. Section 1734 solely to indicate this fact.

§ The on-line version of this article (available at <http://www.mcponline.org>) contains supplemental material.

|| To whom correspondence may be addressed. Tel.: 31-30-2121800; Fax: 31-30-2516464; E-mail: j.denhertog@niob.knaw.nl.

** To whom correspondence may be addressed. Tel.: 31-30-2533789; Fax: 31-30-2518219; E-mail: m.slijper@uu.nl.

REFERENCES

- Salomon, A. R., Ficarro, S. B., Brill, L. M., Brinker, A., Phung, Q. T., Ericson, C., Sauer, K., Brock, A., Horn, D. M., Schultz, P. G., and Peters, E. C. (2003) Profiling of tyrosine phosphorylation pathways in human cells using mass spectrometry. *Proc. Natl. Acad. Sci. U. S. A.* **100**, 443–448
- Blagoev, B., Kratchmarova, I., Ong, S. E., Nielsen, M., Foster, L. J., and Mann, M. (2003) A proteomics strategy to elucidate functional protein-protein interactions applied to EGF signaling. *Nat. Biotechnol.* **21**, 315–318
- Brill, L. M., Salomon, A. R., Ficarro, S. B., Mukherji, M., Stettler-Gill, M., and Peters, E. C. (2004) Robust phosphoproteomic profiling of tyrosine phosphorylation sites from human T cells using immobilized metal affinity chromatography and tandem mass spectrometry. *Anal. Chem.* **76**, 2763–2772
- Thelemann, A., Petti, F., Griffin, G., Iwata, K., Hunt, T., Settinaro, T., Fenyó, D., Gibson, N., and Haley, J. D. (2005) Phosphotyrosine signaling networks in epidermal growth factor receptor overexpressing squamous carcinoma cells. *Mol. Cell. Proteomics* **4**, 356–376
- Blagoev, B., Ong, S. E., Kratchmarova, I., and Mann, M. (2004) Temporal analysis of phosphotyrosine-dependent signaling networks by quantitative proteomics. *Nat. Biotechnol.* **22**, 1139–1145
- Beis, D., and Stainier, D. Y. (2006) *In vivo* cell biology: following the zebrafish trend. *Trends Cell Biol.* **16**, 105–112
- Dooley, K., and Zon, L. I. (2000) Zebrafish: a model system for the study of human disease. *Curr. Opin. Genet. Dev.* **10**, 252–256
- Grunwald, D. J., and Eisen, J. S. (2002) Headwaters of the zebrafish—emergence of a new model vertebrate. *Nat. Rev. Genet.* **3**, 717–724
- Driever, W., Solnica-Krezel, L., Schier, A. F., Neuhaus, S. C., Malicki, J., Stemple, D. L., Stainier, D. Y., Zwartkruis, F., Abdellah, S., Rangini, Z., Belak, J., and Boggs, C. (1996) A genetic screen for mutations affecting embryogenesis in zebrafish. *Development* **123**, 37–46
- Haffter, P., Granato, M., Brand, M., Mullins, M. C., Hammerschmidt, M., Kane, D. A., Odenthal, J., van Eeden, F. J., Jiang, Y. J., Heisenberg, C. P., Kelsch, R. N., Furutani-Seiki, M., Vogelsang, E., Beuchle, D., Schach, U., Fabian, C., and Nusslein-Volhard, C. (1996) The identification of genes with unique and essential functions in the development of the zebrafish, *Danio rerio*. *Development* **123**, 1–36
- Cooper, J. A., Sefton, B. M., and Hunter, T. (1983) Detection and quantification of phosphotyrosine in proteins. *Methods Enzymol.* **99**, 387–402
- Link, V., Shevchenko, A., and Heisenberg, C. P. (2006) Proteomics of early zebrafish embryos. *BMC Dev. Biol.* **6**, 1
- Westerfield, M. (2000) *The Zebrafish Book. A Guide for the Laboratory Use of the Zebrafish (Danio rerio)*, 4th Ed., University of Oregon Press, Eugene, OR
- Gobom, J., Nordhoff, E., Mirgorodskaya, E., Ekman, R., and Roepstorff, P. (1999) Sample purification and preparation technique based on nanoscale reversed-phase columns for the sensitive analysis of complex peptide mixtures by matrix-assisted laser desorption/ionization mass spectrometry. *J. Mass Spectrom.* **34**, 105–116
- Meiring, H. D., van der Heeft, E., ten Hove, G. J., and de Jong, A. P. J. M. (2002) Nanoscale LC-MS[(n)]: technical design and applications to peptide and protein analysis. *J. Sep. Sci.* **25**, 557–568
- Nesvizhskii, A. I., Keller, A., Kolker, E., and Aebersold, R. (2003) A statistical model for identifying proteins by tandem mass spectrometry. *Anal. Chem.* **75**, 4646–4658
- Hokaiwado, N., Asamoto, M., Tsujimura, K., Hirota, T., Ichihara, T., Satoh,

- T., and Shirai, T. (2004) Rapid analysis of gene expression changes caused by liver carcinogens and chemopreventive agents using a newly developed three-dimensional microarray system. *Cancer Sci.* **95**, 123–130
18. Wu, Y., de Kievit, P., Vahlkamp, L., Pijnenburg, D., Smit, M., Dankers, M., Melchers, D., Stax, M., Boender, P. J., Ingham, C., Bastiaensen, N., de Wijn, R., van Alewijk, D., van Damme, H., Raap, A. K., Chan, A. B., and van Beuningen, R. (2004) Quantitative assessment of a novel flow-through porous microarray for the rapid analysis of gene expression profiles. *Nucleic Acids Res.* **32**, e123
 19. van Beuningen, R., van Damme, H., Boender, P., Bastiaensen, N., Chan, A., and Kievits, T. (2001) Fast and specific hybridization using flow-through microarrays on porous metal oxide. *Clin. Chem.* **47**, 1931–1933
 20. Lemeer, S., Jopling, C., Najfi, F., Ruijtenbeek, R., Slijper, M., Heck, A. J., and den Hertog, J. (2007) Protein-tyrosine kinase activity profiling in knock down zebrafish embryos. *PLoS ONE* **2**, e581
 21. Beausoleil, S. A., Jedrychowski, M., Schwartz, D., Elias, J. E., Villen, J., Li, J., Cohn, M. A., Cantley, L. C., and Gygi, S. P. (2004) Large-scale characterization of HeLa cell nuclear phosphoproteins. *Proc. Natl. Acad. Sci. U. S. A.* **101**, 12130–12135
 22. Amanchy, R., Kalume, D. E., Iwahori, A., Zhong, J., and Pandey, A. (2005) Phosphoproteome analysis of HeLa cells using stable isotope labeling with amino acids in cell culture (SILAC). *J. Proteome Res.* **4**, 1661–1671
 23. Rush, J., Moritz, A., Lee, K. A., Guo, A., Goss, V. L., Spek, E. J., Zhang, H., Zha, X. M., Polakiewicz, R. D., and Comb, M. J. (2005) Immunoaffinity profiling of tyrosine phosphorylation in cancer cells. *Nat. Biotechnol.* **23**, 94–101
 24. Mukherji, M., Brill, L. M., Ficarro, S. B., Hampton, G. M., and Schultz, P. G. A. (2006) Phosphoproteomic analysis of the ErbB2 receptor tyrosine kinase signaling pathways. *Biochemistry* **45**, 15529–15540
 25. Zhang, Y., Wolf-Yadlin, A., Ross, P. L., Pappin, D. J., Rush, J., Lauffenburger, D. A., and White, F. M. (2005) Time-resolved mass spectrometry of tyrosine phosphorylation sites in the epidermal growth factor receptor signaling network reveals dynamic modules. *Mol. Cell. Proteomics* **4**, 1240–1250
 26. Tay, T. L., Lin, Q., Seow, T. K., Tan, K. H., Hew, C. L., and Gong, Z. (2006) Proteomic analysis of protein profiles during early development of the zebrafish, *Danio rerio*. *Proteomics* **6**, 3176–3188
 27. Hagel, M., George, E. L., Kim, A., Tamimi, R., Opitz, S. L., Turner, C. E., Imamoto, A., and Thomas, S. M. (2002) The adaptor protein paxillin is essential for normal development in the mouse and is a critical transducer of fibronectin signaling. *Mol. Cell. Biol.* **22**, 901–915
 28. Schaller, M. D., and Parsons, J. T. (1995) pp125FAK-dependent tyrosine phosphorylation of paxillin creates a high-affinity binding site for Crk. *Mol. Cell. Biol.* **15**, 2635–2645
 29. Crawford, B. D., Henry, C. A., Clason, T. A., Becker, A. L., and Hille, M. B. (2003) Activity and distribution of paxillin, focal adhesion kinase, and cadherin indicate cooperative roles during zebrafish morphogenesis. *Mol. Biol. Cell* **14**, 3065–3081
 30. Turner, C. E. (1991) Paxillin is a major phosphotyrosine-containing protein during embryonic development. *J. Cell Biol.* **115**, 201–207
 31. Schaller, M. D., and Schaefer, E. M. (2001) Multiple stimuli induce tyrosine phosphorylation of the Crk-binding sites of paxillin. *Biochem. J.* **360**, 57–66
 32. Hsia, D. A., Mitra, S. K., Hauck, C. R., Streblov, D. N., Nelson, J. A., Ilic, D., Huang, S., Li, E., Nemerow, G. R., Leng, J., Spencer, K. S., Cheresch, D. A., and Schlaepfer, D. D. (2003) Differential regulation of cell motility and invasion by FAK. *J. Cell Biol.* **160**, 753–767
 33. Jopling, C., and den Hertog, J. (2005) Fyn/Yes and non-canonical Wnt signalling converge on RhoA in vertebrate gastrulation cell movements. *EMBO Rep.* **6**, 426–431
 34. Tsai, W. B., Zhang, X., Sharma, D., Wu, W., and Kinsey, W. H. (2005) Role of Yes kinase during early zebrafish development. *Dev. Biol.* **277**, 129–141
 35. Davis, S., Gale, N. W., Aldrich, T. H., Maisonpierre, P. C., Lhotak, V., Pawson, T., Goldfarb, M., and Yancopoulos, G. D. (1994) Ligands for EPH-related receptor tyrosine kinases that require membrane attachment or clustering for activity. *Science* **266**, 816–819
 36. Klein, R. (1999) Bidirectional signals establish boundaries. *Curr. Biol.* **9**, R691–R694
 37. Mellitzer, G., Xu, Q., and Wilkinson, D. G. (1999) Eph receptors and ephrins restrict cell intermingling and communication. *Nature* **400**, 77–81
 38. Cooke, J. E., Kemp, H. A., and Moens, C. B. (2005) EphA4 is required for cell adhesion and rhombomere-boundary formation in the zebrafish. *Curr. Biol.* **15**, 536–542
 39. Mellitzer, G., Xu, Q., and Wilkinson, D. G. (2000) Control of cell behaviour by signalling through Eph receptors and ephrins. *Curr. Opin. Neurobiol.* **10**, 400–408
 40. Xu, Q., Mellitzer, G., Robinson, V., and Wilkinson, D. G. (1999) In vivo cell sorting in complementary segmental domains mediated by Eph receptors and ephrins. *Nature* **399**, 267–271